Coupled-Channel Effects in Collisions between Heavy Ions near the Coulomb Barrier

C. Beck

Abstract With the recent availability of state-of-the-art heavy-ion stable and radioactive beams, there has been a renew interest in the investigation of nuclear reactions with heavy ions. I first present the role of inelastic and transfer channel couplings in fusion reactions induced by stable heavy ions. Analysis of experimental fusion cross sections by using standard coupled-channel calculations is discussed. The role of multi-neutron transfer is investigated in the fusion process below the Coulomb barrier by analyzing ^{32}S+^{90,96}Zr as benchmark reactions. The enhancement of fusion cross sections for ^{32}S+^{96}Zr is well reproduced at sub-barrier energies by NTFus code calculations including the coupling of the neutron-transfer channels following the Zagrebaev semi-classical model. Similar effects for ^{40}Ca+^{90}Zr and ^{40}Ca+^{96}Zr fusion excitation functions are found. The breakup coupling in both the elastic scattering and in the fusion process induced by weakly bound stable projectiles is also shown to be crucial. In this lecture, full coupled-channel calculations of the fusion excitation functions are performed by using the breakup coupling for the more neutron-rich reaction and for the more weakly bound projectiles. I clearly demonstrate that Continuum-Discretized Coupled-Channel calculations are capable to reproduce the fusion enhancement from the breakup coupling in ^{6}Li+^{59}Co.

1 Introduction

Heavy-ion fusion reactions at bombarding energies at the vicinity and below the Coulomb barrier have been widely studied [1, 2, 3, 4, 5]. In low-energy fusion reactions, the very simple one-dimensional barrier-penetration model (1D-BPM) [1, 2] is based upon a real potential barrier resulting from the attractive nuclear and repul-

C. Beck

Institut pluridisciplinaire Hubert Curien, IN$_2$P$_3$-CNRS and Université de Strasbourg - 23, rue du Loess BP 28, F-67037 Strasbourg Cedex 2, France, e-mail: christian.beck@iphc.cnrs.fr

sive Coulomb interactions. For light- and medium-mass nuclei, one only assumes that the di-nuclear system (DNS) fuses as soon as it has reached the region inside the barrier i.e. within the potential pocket. If the system can evolve with a bombarding energy high enough to pass through the barrier and to reach this pocket with a reasonable amount of energy, the fusion process will occur after a complete amalgation of the colliding nuclei forming the compound nucleus (CN). On the other hand, for sub-barrier energies the DNS has not enough energy to pass through the barrier.

In reactions induced by stable beams, the specific role of multi-step nucleon-transfers in sub-barrier fusion enhancement still needs to be investigated in detail both experimentally and theoretically [6, 7, 8, 9, 10, 11, 12, 13, 14]. In a complete description of the fusion dynamics the transfer channels in standard coupled-channel (CC) calculations [2, 8, 10, 14, 15] have to be taken into account accurately. It is known, for instance, that neutron transfers may induce a neck region of nuclear matter in-between the interacting nuclei favoring the fusion process to occur. In this case, neutron pick-up processes can occur when the nuclei are close enough to interact each other significantly [7, 8], if the Q-values of neutron transfers are positive. It was shown that sequential neutron transfers can lead to the broad distributions characteristic of many experimental fusion cross sections. Finite Q-value effects can lead to neutron flow and a build up of a neck between the target and projectile [8]. The situation of this neck formation of neutron matter between the two colliding nuclei could be considered as a "doorway state" to fusion. In a basic view, this intermediate state induced a barrier lowering. As a consequence, it will favor the fusion process at sub-barrier energies and enhance significantly the fusion cross sections. Experimental results have already shown such enhancement of the sub-barrier fusion cross sections due to the neutron-transfer channels with positive Q-values [6, 9].

In reactions induced by weakly bound nuclei and/or by halo nuclei, the influence on the fusion process of coupling both to collective degrees of freedom and to transfer/breakup channels is a key point [3, 4, 5] for the understanding of N-body systems in quantum dynamics [1]. Due to their very weak binding energies, a diffuse cloud of neutrons for ^{6}He or an extended spatial distribution for the loosely bound proton in ^{8}B would lead to larger total reaction (and fusion) cross sections at sub-barrier energies as compared to 1D-BPM model predictions. This enhancement is well understood in terms of the dynamical processes arising from strong couplings to collective inelastic excitations of the target (such as "normal" quadrupole and octupole modes) and projectile (such as soft dipole resonances). However, in the case of reactions where at least one of the colliding nuclei has a sufficiently low binding energy for breakup to become a competitive process, conflicting conclusions were reported [3, 4, 5, 16, 17].

Recent studies with Radioactive Ion Beams (RIB) indicate that the halo nature of ^{6,8}He [18, 19, 20, 21, 22], for instance, does not enhance the fusion probability as anticipated. Rather the prominent role of one- and two-neutron transfers in ^{6,8}He induced fusion reactions was definitively demonstrated. On the other hand, the effect of non-conventional transfer/stripping processes appears to be less significant for stable weakly bound projectiles. Several experiments involving ^{9}Be, ^{7}Li, and ^{6}Li projectiles on medium-mass targets have been undertaken.

Fig. 1 Comparison between the fusion-evaporation (ER) excitation functions of ^{32}S+^{90}Zr (open circles) and ^{32}S+^{96}Zr (points) as a function of the center-of-mass energy. The error barrs of the experimental data taken from Ref. [23] represent purely statistics uncertainties. (Courtesy of H.Q. Zhang)
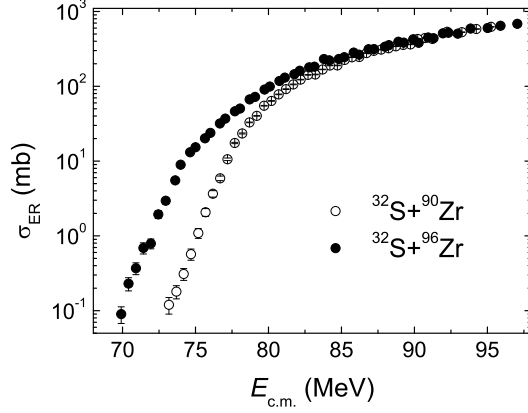
Fig. 2 Ratios of measured fusion cross sections for ^{6}Li and ^{7}Li projectiles with ^{24}Mg, ^{28}Si and ^{59}Co targets as a function of $E_{c.m.}/V_b$. The solid line gives the 1D-BPM prediction while the dotted line shows results obtained from Wong's prescription. (This figure originally shown in Ref. [24] for ^{6,7}Li+^{59}Co has been adapted to display comparisons with other lighter targets [25, 26, 27, 28])
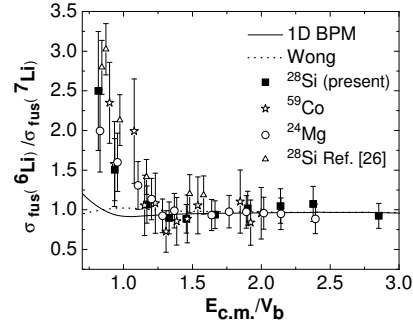
2 Experimental results

In this lecture we first present the role of inelastic and transfer channel couplings in experimental data obtained in fusion reactions induced by stable ^{32}S projectiles [23]. The breakup coupling in both elastic scattering data and in the fusion data are also shown for weakly bound ^{6,7}Li projectiles [24].

2.1 ^{32}S + ^{90}Zr and ^{32}S + ^{96}Zr reactions

In order to investigate the role of neutron transfers we further study ^{32}S + ^{90}Zr and ^{32}S + ^{96}Zr as benchmark reactions. Fig. 1 displays the measured fusion cross sections for ^{32}S + ^{90}Zr (open circles) and ^{32}S + ^{96}Zr (points). We present the analysis of excitation functions of evaporation residues (ER) cross sections recently measured

with high precision (i.e. with small energy steps and good statistical accuracy for these reactions [23]).

The differential cross sections of quasi-elastic scattering (QEL) at backward angles were previously measured by the CIAE group [13]. The analysis of the corresponding BD-QEL barrier distributions (see solid points in Fig. 3) already indicated the significant role played by neutron tranfers in the fusion processes.

In Fig. 3 we introduce the experimental fusion-barrier (BD-Fusion) distributions (see open poins) obtained for the two reactions by using the three-point difference method of Ref. [8] as applied to the data points of Ref. [23] plotted in Fig. 1. It is interesting to note that in both cases the BD-Fusion and BD-QEL barrier distributions are almost identical up to $E_{c.m.} \approx 85$ MeV.

2.2 $^{6}Li + ^{59}Co$ and $^{7}Li + ^{59}Co$ reactions

The fusion excitation functions were measured for the ^{6,7}Li+^{59}Co reactions [24] at the VIVITRON facility of the IPHC Strasbourg and the Pelletron facility of Saõ Paulo by using γ-ray techniques. Their ratios are presented in Fig. 2 with comparisons with other lighter targets [25, 26, 27, 28]. The theoretical curves (1D-BPM [1, 2] and Wong [15] do not take into account the breakup channel coupling that is discussed in one of the following sections in more details.

3 Coupled channel analysis

Analysis of experimental fusion cross sections by using standard CC calculations is first discussed with the emphasis of the role of multi-neutron transfer in the fusion process below the Coulomb barrier for ^{32}S+^{90,96}Zr as benchmark reactions.

## 3.1 $^{32}S + ^{90}Zr$ and $^{32}S + ^{96}Zr$ reactions

A new CC computer code named NTFus [29] taking the neutron transfer channels into account in the framework of the semiclassical model of Zagrebaev [10] has been developed. The effect of the neutron transfer channels yields a fairly good agreement with the data of sub-barrier fusion cross sections measured for ^{32}S + ^{96}Zr, the more neutron-rich reaction [23]. This was initially expected from the positive Q-values of the neutron transfers as well as from the failure of standard CC calculation of quasi-elastic barrier distributions without neutron-transfers coupling [13] as shown by the solid line in Fig. 3(b).

By fitting the experimental fusion excitation function displayed in Fig. 1 with NTFus CC calculation [29], we concluded [30] that the effect of the neutron transfer

channels produces significant enhancement of the sub-barrier fusion cross sections of $^{32}S + ^{96}Zr$ as compared to $^{32}S + ^{90}Zr$. A detailed inspection of the $^{32}S + ^{90}Zr$ fusion data presented in Fig. 1 along with the negative Q-values of their corresponding neutron transfer channels lead us to speculate with the absence of a neutron transfer effect on the sub-barrier fusion for this reaction. With the semiclassical model developed by Zagrebaev [10] we propose to definitively demonstrate the significant role of neutron transfers for the $^{32}S + ^{96}Zr$ fusion reaction by fitting its experimental excitation function with NTFUS code [29] calculations, as shown in Fig. 3.

Fig. 3 Barrier distributions (BD) from the fusion ER (open circles) cross sections [23], plotted in Fig.1, and quasielastic scattering (solid circles) cross sections [13] for $^{32}S+^{90}Zr$ (a) and $^{32}S+^{96}Zr$ (b). The dashed and solid black lines represent uncoupled calculations (1D-BPM) and the CC calculations without neutron transfer coupling. The red dash-dotted line represents the CC calculations with neutron transfer coupling for the $^{32}S+^{96}Zr$ reaction. (Courtesy of H.Q. Zhang)
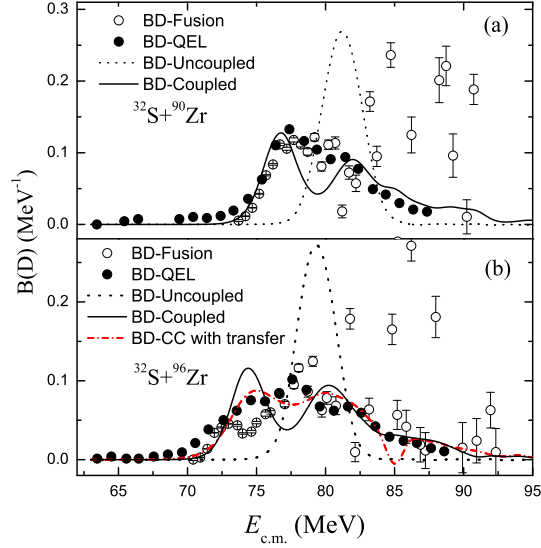
The new oriented object NTFUS code [29], using the Zagrebaev model [10] was implemented (at the CIAE) in C++, using the compiler of ROOT [31], following the basic equations of Ref. [32]. Let us first remind the values chosen for the deformation parameters and the excitation energies that are given in Refs. [2, 33, 34] (see Tables given in [30] for more details). The quadrupole vibrations of both the ^{90}Zr and ^{96}Zr are weak in energy; they lie at comparable energies. The ^{96}Zr nucleus presents a complicated situation [35]: its low-energy spectrum is dominated by a 2^+ state at 1.748 MeV and by a very collective [B(E3;$3^- \rightarrow 0^+$) = 51 W.u.] 3^- state at 1.897 MeV. CC calculations explained the larger sub-barrier enhancement as due mainly to the strong octupole vibration of the 3^- state in $^{36}S + ^{96}Zr$ [36]. However, the agreement is not so satisfactory below the barrier for $^{32}S + ^{96}Zr$ (see solid line of Fig. 3.b), as well as for $^{40}Ca + ^{96}Zr$ [9] and, therefore, there is the need to take neutron transfers into account.

The main functions of the code NTFUS are designed to calculate the fusion excitation functions with normalized barrier distribution (based on experimental data) given by CCFULL [15], we take the dynamical deformations into account. In order to introduce the role of neutron transfers, the NTFUS code [29] applies the Za-

grebaev model [10] to calculate the fusion cross sections $\sigma_{fus}(E)$ as a function of center-of-mass energy E. Then the fusion excitation function can be derived using the following formula [10]:

$$T_l(E) =$$

$$\int f(B) \frac{1}{N_{tr}} \sum_k \int_{-E}^{Q_0(k)} \alpha_k(E,l,Q) \times P_{HW}(B,E+Q,l) dQ dB. \qquad (1)$$

and

$$\sigma_{fus}(E) = \frac{\pi \hbar^2}{2\mu E} \sum_{l=0}^{l_{cr}} (2l+1) T_l(E). \qquad (2)$$

where $T_l(E)$ are the transmission coefficients, E is the energy given in the center-of-mass system, B and $f(B)$ are the barrier height and the normalized barrier distribution function, P_{HW} is the usual Hill-Wheeler formula. l is the angular momentum whereas l_{cr} is the critical angular momentum as calculated by assuming no coupling (well above the barrier). $\alpha_k(E,l,Q)$ and $Q_0(k)$ are, respectively, the probabilities and the Q-values for the transfers of k neutrons. And $1/N_{tr}$ is the normalization of the total probability taking into account the neutron transfers.

The NTFUS code [29] uses the ion-ion potential between two deformed nuclei as developed by Zagrebaev and Samarin in Ref. [32]. Either the standard Woods-Saxon form of the nuclear potential or a proximity potential [37] can be chosen. The code is also able to predict fusion cross sections for reactions induced by halo projectiles [30]; for instance ^{6}He + ^{64}Zn [22, 38]. In the following, only comparisons for ^{32}S + ^{90}Zr and ^{32}S + ^{96}Zr are discussed.

For the high-energy part of the ^{32}S + ^{90}Zr excitation function, one can notice a small over-estimation of the fusion cross sections at energies above the barrier up to the point used to calculate the critical angular momentum. This behavior can be observed at rather high incident energies - i.e. between about 82 MeV and 90 MeV (shown as the dashed line in Fig. 3.(a) for ^{32}S + ^{90}Zr reaction). We want to stress that the corrections do not affect our conclusions that the transfer channels have a predominant role below the barrier for ^{32}S + ^{96}Zr reaction, as shown by the dotted-dashed red curve in Fig. 3.(b).

As expected, we obtain a good agreement with calculations not taking any neutron transfer coupling into account for ^{32}S + ^{90}Zr as shown by the solid line of Fig. 3.(a) (the dashed line are the results of calculations performed without any coupling). On the other hand, there is no significant over-estimation at sub-barrier energies. As a consequence, it is possible to observe the strong effect of neutron transfers on the fusion for the ^{32}S + ^{96}Zr reaction at sub-barrier energies. Moreover, the barrier distribution function $f(B)$ extracted from the data contains the information of the neutron transfers. These information are also contained in the transmission coefficients, which are the most important parameters for the fusion cross sections to be calculated accurately. The $f(B)$ function as calculated with the three-point formula [8] will mimic the differences induced by the neutron transfer taking place in

sub-barrier energies where the cross section variations are very small (only visible if a logarithm scale is employed for the fusion excitation function). It is interesting to note that the Zagrebaev model [10] implies a modification of the Hill-Wheeler probability and does not concern the barrier distribution function $f(B)$. Finally, the code allows us to perform each calculation by taking the neutron transfers into account or not.

The calculation with the neutron transfer effect is performed up to the channel +4n (k=4), but we have seen that we obtain the same overall agreement with data up to channels +5n and +6n [30]. As we can see on Fig. 3.(b), the solid line representing standard CC calculations without the neutron transfer coupling (the dotted line is given for uncoupled calculations) does not fit the experimental data well at sub-barrier energies. On the other hand, the dotted line displaying NTFus calculations taking the neutron transfer coupling into account agrees perfectly well with the data. As expected, the Zagrebaev semiclassical model's correction applied at sub-barrier energies enhances the calcutated cross sections. Moreover, it allows to fit the data reasonably well and therefore illustrates the strong effect of neutron transfers for the fusion of ^{32}S + ^{96}Zr at subbarrier energies.

The present full CC analysis of ^{32}S + ^{96}Zr fusion data [23, 30] using NTFus [29] confirms perfectly well first previous CC calculations [10] describing well the earlier ^{40}Ca + ^{90,96}Zr fusion data [9] and, secondly, very recent fragment-γ coincidences measured for ^{40}Ca + ^{96}Zr multi-neutron transfer channels [35].

3.2 ^{6}Li + ^{59}Co and ^{7}Li + ^{59}Co reactions

For reactions induced by weakly bound nuclei [16, 17, 25, 26, 27, 28, 39, 40, 41] and exotic nuclei [18, 19, 20, 21, 22, 38, 42, 43, 44, 45, 46], the breakup channel is open and plays a key role in the fusion process near the Coulomb barrier similarly to the transfer-channel coupling described in the previous section. It is therefore appropriate to use the Continuum-Discretized Coupled-Channel (CDCC) approach [47, 48, 49, 50] to describe the influence of the breakup channel in both the elastic scattering and the fusion process at sub-barrier energies.

Theoretical calculations (including CDCC predictions given in Refs. [47, 49] indicate only a small enhancement of total fusion for the more weakly bound ^{6}Li below the Coulomb barrier (see curves of Fig.2), with similar cross sections for both ^{6,7}Li+^{59}Co reactions at and above the barrier [24]. It is interesting to notice, however, that the same conclusions have been reached for other targets such as ^{24}Mg [26] and ^{28}Si [25, 27, 28] as can be clearly seen in the plot of Fig. 2. Thess results are consistent with rather low breakup cross sections measured for the ^{6,7}Li+^{59}Co reactions even at incident energies larger than the Coulomb barrier [39, 40, 41]. But the coupling of the breakup channel is extremely important for the CDCC analysis of the angular distributions of the elastic scattering [47] as shown in Fig. 4 for ^{6}Li+^{59}Co. The curves show the results of calculations with (solid lines) and with-

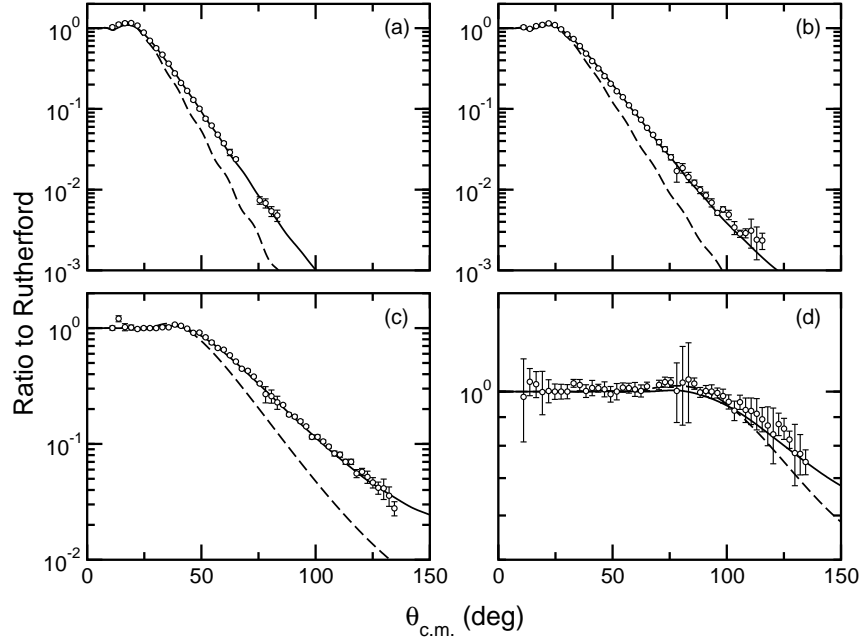**Fig. 4** Ratios of the elastic scattering cross-sections to the Rutherford cross sections as a function of c.m. angle for the ^{6}Li+^{59}Co system [47]. The curves correspond to CDCC calculations with (solid lines) and without (dashed lines) ^{6}Li $\rightarrow \alpha + d$ breakup couplings to the continuum for incident ^{6}Li energies of (a) 30 MeV, (b) 26 MeV, (c) 18 MeV and (d) 12 MeV. (This figure has been adapted from the work of Ref. [47])

out (dashed lines) ^{6,7}Li $\rightarrow \alpha + d,t$ breakup couplings. The main conclusion is that effect of breakup on the elastic scattering is stronger for ^{6}Li than ^{7}Li.

A more detailed investigation of the breakup process in the ^{6}Li+^{59}Co reaction with particle coincidence techniques is now proposed to discuss the interplay of fusion and breakup processes. Coincidence data compared to three-body kinematics calculations reveal a way how to disentangle the contributions of breakup, incomplete fusion and/or transfer-reemission processes [39, 40, 41].

Fig. 5 displays experimental (full rectangles) and theoretical angular distributions (solid lines) for the sequential (SBU) and direct (DBU) projectile breakup processes at the two indicated bombarding energies for the ^{6}Li+^{59}Co reaction. In the CDCC calculations the $\alpha + d$ binning scheme is appropriately altered to accord exactly with the measured continuum excitation energy ranges. For this reaction it was not necessary to use a sophisticated four-body CDCC framework. The CDCC cross sections [47] are in agreement with the experimental ones [16, 40, 41], both in shapes and magnitudes within the uncertainties. The relative contributions of the ^{6}Li SBU and DBU to the incomplete fusion/transfer process has been discussed in great details in Refs. [39, 40, 41] by considering the corresponding lifetimes obtained by using a semi-classical approach fully described in a previous publication [39]. We con-

Fig. 5 Experimental [39, 40, 41] and theoretical CDCC [30] angular distributions for the SBU and DBU projectile breakup processes (see text for details) obtained at E_{lab} = 25.5 MeV and 29.6 MeV for ^{6}Li+^{59}Co. The chosen experimental continuum excitation energy ranges are given. (Courtesy of F.A, Souza)
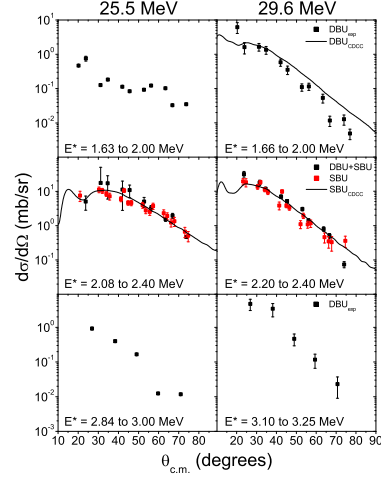
clude that the flux diverted from complete fusion to incomplete fusion would arise essentially from DBU processes via high-lying continuum (non-resonant) states of ^{6}Li; this is due to the fact that both the SBU mechanism and the low-lying DBU processes from low-lying resonant ^{6}Li states occur at large internuclear distances [39, 40, 41]. Work is in progress to study incomplete fusion for ^{6}Li+^{59}Co within a newly developed 3-dimensional classical trajectory model [51].

3.3 Coupled-channel calculations for reactions induced by halo nuclei

As far as exotic halo projectiles are concerned we have initiated a systematic study of ^{8}B and ^{7}Be induced reactions data [52] with an improved CDCC method [48]. Fig. 6 displays the analysis of the elastic scattering for the ^{7}Be+^{58}Ni system [52]. The curves correspond to CDCC calculations with (solid lines) and without (dashed lines) ^{7}Be $\rightarrow \alpha + ^3$He breakup couplings to the continuum. The ^{6}Li and ^{7}Be calculations were similar, but with a finer continuum binning for ^{7}Be. As compared to ^{7}Be+^{58}Ni (similar to ^{6,7}Li+^{58,64}Ni) the CDCC analysis of ^{8}B+^{58}Ni reaction [48] while exhibiting a large breakup cross section (consistent with the systematics) is rather surprising as regards the consequent weak coupling effect found to be particularly small on the near-barrier elastic scattering.

Recently, the scattering process of ^{17}F from ^{58}Ni target was investigated [43] slightly above the Coulomb barrier and total reaction cross sections were extracted from the Optical-Model analysis. The small enhancement as compared to the reference (tightly bound) system ^{16}O+^{58}Ni is here related to the low binding energy
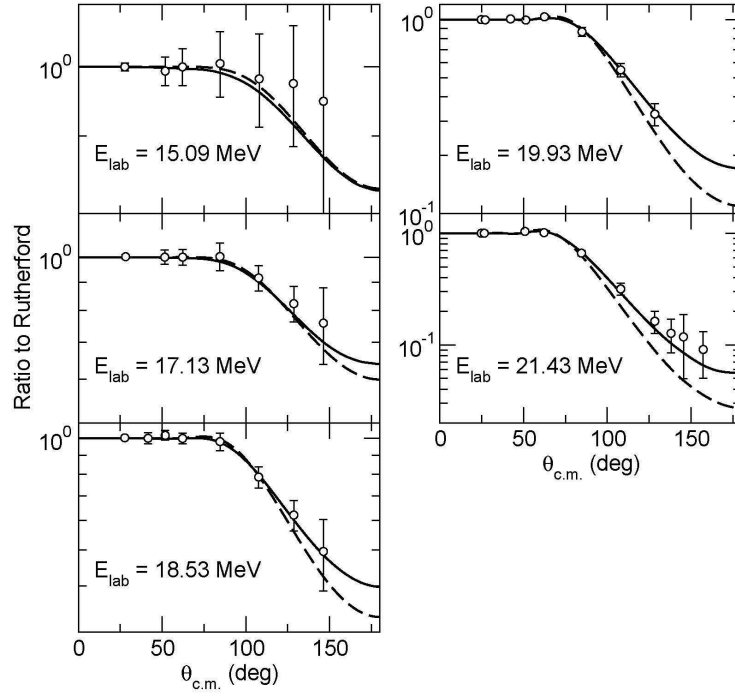
Fig. 6 Ratios of the elastic scattering cross-sections to the Rutherford cross sections as a function of c.m. angle for the ^{7}Be+^{58}Ni system [52] for incident ^{7}Be energies of (a) 15.09 MeV, (b) 17.13 MeV, (c) 18.53 MeV (d) 19.93 MeV and (e) 21.43 MeV. The solid and dashhed curves denote full and no coupling to the continuum. (This figure has been adapted from the work of Ref. [17])

of the ^{17}F valence proton. This moderate effect is mainly triggered from a transfer effect, as observed for the 2n-halo ^{6}He [18, 19] and the 1n-halo ^{11}Be [42] in contrast to the 1p-halo ^{8}B+^{58}Ni reaction where strong enhancements are trigerred from a breakup process [45].

4 Summary, conclusions and outlook

We have investigated the fusion process (excitation functions and extracted barrier distributions [23]) at near- and sub-barrier energies for the two neighbouring reactions ^{32}S + ^{90}Zr and ^{32}S + ^{96}Zr. For this purpose a new computer code named NTFus [29] has been developped by taking the coupling of the multi-neutron transfer channels into account by using the semiclassical model of Zagrebaev [10].

The effect of neutron couplings provides a fair agreement with the present data of sub-barrier fusion for ^{32}S + ^{96}Zr. This was initially expected from the positive Q-values of the neutron transfers as well as from the failure of previous CC calculation of quasi-elastic barrier distributions without coupling of the neutron transfers [13]. With the agreement obtained by fitting the present experimental fusion excitation function and the CC calculation at sub-barrier energies, we conclude that the effect of the neutron transfers produces a rather significant enhancement of the sub-barrier fusion cross sections of ^{32}S + ^{96}Zr as compared to ^{32}S + ^{90}Zr. At this point we did not try to reproduce the details of the fine structures observed in the fusion barrier distributions. We believe that to achieve this final goal it will first be necessary to measure the neutron transfer cross sections to provide more information on the coupling strength of neutron transfer because its connection with fusion is not yet fully understood [35].

In the second part of this lecture, we have studied the breakup coupling on elastic scattering and fusion by using the CDCC approach with a particular emphasis on a very detailed analysis of the ^{6}Li+^{59}Co reaction. The CDCC formalism, with continuum–continuum couplings taken into account, is probably one of the most reliable methods available nowadays to study reactions induced by exotic halo nuclei, although many of them have added complications like core excitation and three-body structure. The respective effects of transfer/breakup are finally outlined for reactions induced by $1p$-halo, $1n$-halo and $2n$-halo nuclei.

The complexity of such reactions, where many processes compete on an equal footing, necessitates kinematically and spectroscopically complete measurements [53], i.e. ones in which all processes from elastic scattering to fusion are measured simultaneously, providing a technical challenge in the design of broad range detection systems. A full understanding of the reaction dynamics involving couplings to the breakup and nucleon-transfer channels will need high-intensity RIB and precise measurements of elastic scattering, fusion and yields leading to the breakup itself. A new experimental program with SPIRAL beams and medium-mass targets is getting underway at GANIL.

References

1. A.B. Balantekin and N. Takigawa, Rev. Mod. Phys. **70**, 77 (1998); arXiv:**nucl-th/9708036** (1997).
2. M. Dasgupta, D.J. Hinde, N. Rowley, and A.M. Stefanini, Annu. Rev. Nucl. Part. Sci. **48**, 401 (1998).
3. J.F. Liang and C. Signorini, Int. J. Mod. Phys. E **14**, 1121 (2005); arXiv:**nucl-ex/0504030** (2005).
4. L.F. Canto, P.R.S. Gomes, R. Donangelo, and M.S. Hussein, Phys. Rep. **424**, 1 (2006).
5. N. Keeley, R. Raabe, N. Alamanos, and J.-L. Sida, Prog. Part. Nucl. Phys. **59**579 (2007); arXiv:**nucl-th/0702038** (2007).
6. R. Pengo, D. Evers, K.E.G. Lobner, U. Quade, K. Rudolph, S.J. Skorka, and I. Weidl, Nucl. Phys. A **411**, 256 (1983).
7. P.H. Stelson, Phys. Lett. B **205**, 190 (1988).
8. N. Rowley, G.J. Thompson, and M.A. Nagarajan, Phys. Lett. B **282**, 276 (1992).
9. H. Timmers, D. Ackermann, S. Beghini, L. Corradi, J.H. He, G. Montagnoli, F. Scarlassara, A.M. Stefanini, and N. Rowley, Nucl. Phys. **A633**, 421 (1998).
10. V.I. Zagrebaev, Phys. Rev. C **67**, 061601 (2003).
11. A.M. Stefanini, F. Scarlassara, S. Beghini, G. Montagnoli, R. Silvestri, M. Trotta, B.R. Behera, L. Corradi, E. Fioretto, A. Gadea, Y.W. Wu, S. Szilner, H.Q. Zhang, Z.H. Liu, M. Ruan, F. Yang, and N. Rowley, Phys. Rev. C **73**, 034606 (2006).
12. A.M. Stefanini, B.R. Behera, S. Beghini, L. Corradi, E. Fioretto, A. Gadea, G. Montagnoli, N. Rowley, F. Scarlassara, S. Szilner, and M. Trotta, Phys. Rev. C **76**, 014610 (2007).
13. F. Yang, C.J. Lin, X.K. Wu, H.Q. Zhang, C.L. Zhang, P. Zhou, and Z.H. Liu, Phys. Rev. C **77**, 014601 (2008).
14. Sunil Kalkal, S. Mandal, N. Madhavan, E. Prasad, Shashi Verma, A. Jhingan, Rohit Sandal, S. Nath, J. Gehlot, B.R. Behera, Mansi Saxena, Savi Goyal, Davinder Siwal, Ritika Garg, U.D. Pramanik, Suresh Kumar, T. Varughese, K.S. Golda, S. Muralithar, A.K. Sinha, and R. Singh, Phys. Rev. C **81**, 044610 (2010).
15. K. Hagino, N. Rowley, and A.T. Kruppa, Comput. Phys. Commun. **123**, 143 (1999); arXiv:**nucl-th/9903074** (1999).
16. C. Beck, Nucl. Phys. A **787**, 251 (2007); arXiv:**nucl-ex/0701073** (2007); arXiv:**nucl-th/0610004** (2006).
17. C. Beck, N. Rowley, P. Papka, S. Courtin, M. Rousseau, F.A. Souza, N. Carlin, R. Liguori Neto, M.M. de Moura, M.G. Del Santo, A.A.P. Suaide, M.G. Munhoz, E.M. Szanto, A. Szanto de Toledo, N. Keeley, A. Diaz-Torres, and K. Hagino, Nucl. Phys. A **834**, 440 (2010); arXiv:**0910.1672** (2010).
18. A. Di Pietro, P. Figuera, F. Amorini, C. Angulo, G. Cardella, S. Cherubini, T. Davinson, D. Leanza, J. Lu, H. Mahmud, M. Milin, A. Musumarra, A. Ninane, M. Papa, M.G. Pellegriti, R. Raabe, F. Rizzo, C. Ruiz, A.C. Shotter, N. Soic, and S. Tudisco, Phys. Rev. C **69**, 044601 (2004).
19. A. Navin, V. Tripathi, Y. Blumenfeld, V. Nanal, C. Simenel, J.M. Casandjian, G. de France, R. Raabe, D. Bazin, A. Chatterjee, M. Dasgupta, S. Kailas, R.C. Lemmon, K. Mahata, R.G. Pilay, E.C. Pollacco, K. Ramachandran, M. Rejmund, A Shrivastava, J.L. Sida, and E. Tryggestad, Phys. Rev. C **70**, 044601 (2004).
20. A. Chatterjee, A. Navin, A. Shrivastava, S. Bhattacharyya, M. Rejmund, N. Keeley, V. Nanal, J. Nyberg, R. G. Pillay, K. Ramachandran, I. Stefan, D. Bazin, D. Beaumel, Y. Blumenfeld, G. de France, D. Gupta, M. Labiche, A. Lemasson, R. Lemmon, R. Raabe, J. A. Scarpaci, C. Simenel, and C. Timis, Phys. Rev. Lett. **101**, 032701 (2008).
21. A. Lemasson, Shrivastava, A. Navin, M. Rejmund, N. Keeley, V. Zelevinsky, S. Bhattacharyya, A. Chatterjee, G. de France, B. Jacquot, V. Nanal, R.G. Pillay, R. Raabe, and C. Schmitt, Phys. Rev. Lett. **103**, 232701 (2009).
22. V. Scuderi, A. Di Pietro, P. Figuera, M. Fisichella, F. Amorini, C. Angulo, G. Cardella, E. Casarejos, M. Lattuada, M. Milin, A. Musumarra, M. Papa, M. G. Pellegriti, R. Raabe, F. Rizzo, N. Skukan, D. Torresi, and M. Zadro, Phys. Rev. C **84**, 064604 (2011).

23. H.Q. Zhang, C.J. Lin, F. Yang, H.M. Jia, X.X. Xu, F. Jia, Z.D. Wu, S.T. Zhang, Z.H. Liu, A. Richard, C. Beck, Phys. Rev. C **82**, 054609 (2010); arXiv: **1005.0727** (2010).
24. C. Beck, F.A. Souza, N. Rowley, S.J. Sanders, N. Aissaoui, E.E. Alonso, P. Bednarczyk, N. Carlin, S. Courtin, A. Diaz-Torres, A. Dummer, F. Haas, A. Hachem, K. Hagino, F. Hoellinger, R.V.F. Janssens, N. Kintz, R. Liguori Neto, E. Martin, M.M. Moura, M.G. Munhoz, P. Papka, M. Rousseau, A. Sanchez i Zafra, O. Stezowski, A.A. Suaide, E.M. Szanto, A. Szanto de Toledo, S. Szilner, and J.Takahashi, Phys. Rev. C **67**, 054602 (2003); arXiv:nucl-ex/**0411002**(2004).
25. M. Sinha, H. Majumdar, P. Basu, Subinit Roy, R. Bhattacharya, M. Biswas, M.K. Pradhan, and S. Kailas, Phys. Rev. C **78**, 027601 (2008); arXiv:**nucl-ex:0805.0953** (2008).
26. M. Ray, A. Mukherjee, M.K. Pradhan, Ritesh Kshetri, M. Saha Sarkar, R. Palit, I. Majumdar, P.K. Joshi, H.C. Jain, and B. Dasmahapatra, Phys. Rev. C **78**, 064617 (2008); arXiv:**nucl-ex:0805.0953** (2008).
27. A. Pakou, K. Rusek, N. Alamanos, X. Aslanoglou, M. Kokkoris, A. Lagoyannis, T.J. Mertz-imekis, A. Musumarra, N.G. Nicolis, D. Pierroutsakou, and D. Roubos, Eur. Phys. J. A **39**, 187 (2009).
28. M. Sinha, H. Majumdar, P. Basu, Su. Roy, R. Bhattacharya, M. Biswas, M.K. Pradhan, R. Palit, I. Mazumdar, and S. Kailas, Eur. Phys. J. A **44**, 403 (2010).
29. H.Q. Zhang, H.Q. Zhang, C.L. Zhang, H.M. Jia, C.J. Lin, F. Yang, Z.H. Liu, Z.D. Wu, F. Jia, X.X. Xu, A. Richard, A.K. Nasirov, G. Mandaglio, M. Manganaro, G. Giardina, and K. Hagino, AIP Conf. Proc. **1235**, 50 (2010).
30. A. Richard, C. Beck, and H.Q. Zhang, EPJ Web of Conferences **17**, 08005 (2011); arXiv:**1104.5333** (2011).
31. http://root.cern.ch, website of ROOT.
32. V.I. Zagrebaev and V.V. Samarin, Physics of Atomic Nuclei **67** No.8, 1462 (2004).
33. S. Raman, C.W. Nestor, and P. Tikkanen, At. Data Nucl. Data Tables **78**, 1 (2001).
34. T. Kebedi and R.H. Spear. At. Data Nucl. Data Tables **89**, 77 (2005).
35. L. Corradi, S. Szilner, G. Pollarolo, G. Colo, P. Mason, E. Farnea, E. Fioretto, A. Gadea, F. Haas, D. Jelavic-Malenica, N. Marginean, C. Michelagnoli, G. Montagnoli, D. Montanari, F. Scarlassara, N. Soic, A.M. Stefanini, C.A. Ur, J.J. Valiente-Dobon, Phys. Rev. C **84**, 034603 (2011).
36. A.M. Stefanini, L. Corradi, A.M. Vinodkumar, F. Yang, F. Scarlassara, G. Montagnoli, S. Beghini, M. Bisogno, Phys. Rev. C **62**, 014601 (2000).
37. J. Blocki, J. Randrup, W.J. Swiatecki, and C. F. Tsang, Annals of Physics **105**, 427 (1977).
38. M. Fisichella, V. Scuderi, A. Di Pietro, P. Figuera, M. Lattuada, C. Marchetta, M. Milin, A. Musumarra, M.G. Pellegriti, N. Skukan, E. Strano, D. Torresi, and M. Zadro, J. Phys.: Conf. Ser. **282**, 012014 (2011).
39. F.A. Souza, C. Beck, N. Carlin, N. Keeley, R. Liguori Neto, M.M. de Moura, M.G. Munhoz, M.G. Del Santo, A.A.P. Suaide, E.M. Szanto, and A.Szanto de Toledo, Nucl. Phys. A **821**, 36 (2009); arXiv:**0811.4556** (2008).
40. F.A. Souza, N. Carlin, C. Beck, N. Keeley, A. Diaz-Torres, R. Liguori Neto, C. Siqueira-Mello, M.M. de Moura, M.G. Munhoz, R.A.N. Oliveira, M.G. Del Santo, A.A.P. Suaide, E.M. Szanto, and A. Szanto de Toledo, Nucl. Phys. A **834**, 420 (2010); arXiv:**0910.0342** (2010).
41. F.A. Souza, N. Carlin, C. Beck, N. Keeley, A. Diaz-Torres, R. Liguori Neto, C. Siqueira-Mello, M.M. de Moura, M.G. Munhoz, R.A.N. Oliveira, M.G. Del Santo, A.A.P. Suaide, E.M. Szanto, and A. Szanto de Toledo, Eur. Phys. J. A **44**, 181 (2010); arXiv:**0909.5556** (2009).
42. A. Di Pietro, G. Randisi, V. Scuderi, L. Acosta, F. Amorini, M.J.G. Borge, P. Figuera, M. Fisichella, L.M. Fraile, J. Gomez-Camacho, H. Jeppesen, M. Lattuada, I. Martel, M. Milin, A. Musumarra, M. Papa, M.G. Pellegriti, F. Perez-Bernal, R. Raabe, F. Rizzo, D. Santonocito, G. Scalia, O. Tengblad, D. Torresi, A.M. Vidal, D. Voulot, F. Wenander, and M. Zadro, Phys. Rev. Lett. **105**, 022701 (2010).
43. M. Mazzocco, C. Signorini, D. Pierroutsakou, T. Glodariu, C. Boiano, F. Farinon, A. Di Pietro, P. Figuera, D. Filipescu, L. Fortunato, A. Guglielmetti, G. Inglima, M. La Commara, M. Lattuada, P. Lotti, C. Mazzocchi, P. Molini, A. Musumarra, A. Pakou, C. Parascandolo, N. Patronis, M. Romoli, M. Sandoli, V. Scuderi, F. Soramel, L. Stroe, D. Torresi, E. Vardaci, and A. Vitturi, Phys. Rev. C **82**, 054604 (2010).

44. Z. Kohley, F. Liang, D. Shapira, R.L. Varner, C.J. Gross, J.M. Allmond, A.L. Caraley, E.A. Coello, F. Favela, K. Lagergren, and P.E. Mueller, Phys. Rev. Lett. **107**, 202701 (2011).
45. E.F. Aguilera and J.J. Kolata, Phys. Rev. C **85**, 014603 (2012).
46. M.J. Rudolph, Z.Q. Gosser, K. Brown, S. Hudan, R.T. de Souza, A. Chbihi, B. Jacquot, M. Famiano, J.F. Liang, D. Shapira, and D. Mercier, Phys. Rev. C **85**, 024605 (2012).
47. C. Beck, N. Keeley, and A. Diaz-Torres, Phys. Rev. C **75**, 054605 (2007); arXiv:**nucl-th/0703085** (2007).
48. N. Keeley, R.S. Mackintosh, and C. Beck, Nucl. Phys. A **834**, 792 (2010).
49. A. Diaz-Torres, I.J. Thompson, C. Beck, Phys. Rev. C **68**, 044607 (2003); arXiv:**nucl-th/0307021** (2003).
50. C. Beck, N. Rowley, P. Papka, S. Courtin, M. Rousseau, F.A. Souza, N. Carlin, F. Liguori Neto, M.M. De Moura, M.G. Del Santo, A.A.I. Suade, M.G. Munhoz, E.M. Szanto, A. Szanto De Toledo, N. Keeley, A. Diaz-Torres, and K. Hagino, Int. J. Mod. Phys. **E20**, 943 (2011); arXiv:**1009.1719** (2010).
51. A. Diaz-Torres, D.J. Hinde, J.A. Tostevin, M. Dasgupta, L.R. Gasques, Phys. Rev. Lett. **98**, 152701 (2007); arXiv:**nucl-th/0703041** (2007).
52. E.F. Aguilera, E.F. Aguilera, E. Martinez-Quiroz, D. Lizcano, A. Gomez-Camacho, J.J. Kolata, L.O. Lamm, V. Guimaraes, R. Lichtenthaler, O. Camargo, F.D. Becchetti, H. Jiang, P.A. DeYoung, P.J. Mears, and T.L.Belyaeva, Phys. Rev. C **79**, 021601 (2009).
53. P. Papka and C. Beck, Clusters in Nuclei, Vol. 2 (Ed.) C. Beck, Lecture Notes in Physics **848**, 299 (2012).